

Local heat flux and energy loss in a 2D vibrated granular gas

Olaf Herbst, Peter Müller, and Annette Zippelius

Institut für Theoretische Physik, Georg-August-Universität, D-37077 Göttingen, Germany

(Dated: November 15, 2018)

Abstract

We performed event-driven simulations of a two-dimensional granular gas between two vibrating walls and directly measured the local heat flux and energy dissipation rate in the stationary state. Describing the local heat flux as a function of the coordinate x in the direction perpendicular to the driving walls, we use a generalization of Fourier's law, $q(x) = \kappa \nabla T(x) + \mu \nabla \rho(x)$, to relate the local heat flux to the local gradients of the temperature and density. This *ansatz* accounts for the fact that density gradients also generate heat flux, not only temperature gradients. The transport coefficients κ and μ are assumed to be independent of x , and we check the validity of this assumption in the simulations. Both κ and μ are determined for different system parameters, in particular, for a wide range of coefficients of restitution. We also compare our numerical results to existing hydrodynamic theories. Agreement is found for κ for very small inelasticities only. Beyond this region, κ and μ exhibit a striking non-monotonic behavior.

Driven granular gases have attracted much attention in recent years [1, 2, 3, 4, 5]. This is partly because in these systems, energy loss in inelastic collisions is eventually balanced by energy input from the driving so that a stationary state can be attained. In physically realistic models, the driving usually acts at the boundaries of the system, e.g. in terms of shearing forces or vibrating walls. Thus, maintaining a stationary state requires a subtle and well-balanced mechanism to transfer energy from the system’s boundaries to its interior. The local energy (or heat) flux and the local energy-dissipation rate are therefore at the heart of every hydrodynamic description [4, 6, 7, 8, 9] of the stationary state of driven granular gases.

Fourier’s law states for elastic systems that the heat current is proportional to the local temperature gradient, the proportionality constant being the thermal conductivity κ [10]. For inelastic systems there is an additional contribution to the heat current from density gradients [6]. The corresponding transport coefficient μ has no analog in elastic systems. Theoretical approaches start from the Boltzmann–Enskog equation to account for these effects. Jenkins and Richman [6] have used Grad’s moment expansion to compute the heat flux for small inelasticity, whereas Dufty et al. [7] have pushed kinetic models using a *stosszahl ansatz* to simplify the collision operator. MD simulations have been performed by Soto et al. [11] to study μ for a granular gas on a vibrated plane in the dilute limit.

In this paper we study the local heat flux and local energy-loss rate, as well as the transport coefficients κ and μ for a driven granular gas in 2 dimensions. To do so, we perform event-driven simulations for the dynamics of N identical inelastic smooth hard disks of diameter a and mass m which are confined to a rectangular box with edges of length L_x and L_y . Periodic boundary conditions are imposed in the y -direction, and the gas is driven through the walls perpendicular to the x -direction, see Fig. 1 for a typical snapshot. The left and right wall vibrate in an idealized saw-tooth manner, characterized by the driving velocity $v_{\text{drive}} > 0$: Upon a collision of a particle with the left/right wall at $x = \mp L_x/2$, its x -component of the velocity changes according to $-2v_x \pm v_{\text{drive}}$, see also [12]. Inelastic inter-particle collisions are modeled using a constant coefficient of normal restitution $\alpha \in]0, 1[$ according to $\hat{\mathbf{n}} \cdot \mathbf{v}'_{12} = -\alpha \hat{\mathbf{n}} \cdot \mathbf{v}_{12}$. Here, $\hat{\mathbf{n}}$ denotes the unit vector of the particles’ relative center-of-mass positions, and \mathbf{v}_{12} , resp. \mathbf{v}'_{12} are the pre-, resp. post-collisional relative center-of-mass velocities.

A simple estimate in [12] yields for the spatially averaged granular temperature $T_0 = N^{-1} \sum_{i=1}^N m \mathbf{v}_i^2 / 2$ in the stationary state

$$\frac{T_0}{m v_{\text{drive}}^2 / \varepsilon^2} \approx \left(\frac{2}{\pi} \right)^3 \psi^{-2} \left(1 + \sqrt{1 + (\pi/2)^2 \varepsilon \psi} \right)^2. \quad (1)$$

Here $\varepsilon := 1 - \alpha^2$ and $\psi := \sqrt{2} \chi \lambda$ are dimensionless parameters. The latter involves the pair correlation at contact χ of the corresponding elastic system and the line density $\lambda := N/L_y$.

In the following discussion of heat flux and dissipation we will, inter alia, be interested in a *scaling limit* $\varepsilon \downarrow 0$ towards an elastic system. In order to prevent the system from heating up indefinitely when switching off dissipation, we also need to scale the driving velocity $v_{\text{drive}} =: \varepsilon v_0$, where v_0 is fixed. Hence, the driving vanishes in the elastic scaling limit, and the spatially averaged temperature reaches a finite value, approximately given by $T_0 \approx (2/\pi)^3 (\chi \lambda)^{-2} m v_0^2$ according to Eq. (1).

Locally, the translational energy changes due to collisions as well as due to free streaming of the particles in between collisions. The latter gives rise to a kinetic contribution to the heat current, \mathbf{q}^{kin} , whereas the collisions are responsible for the energy loss ζ as well as for

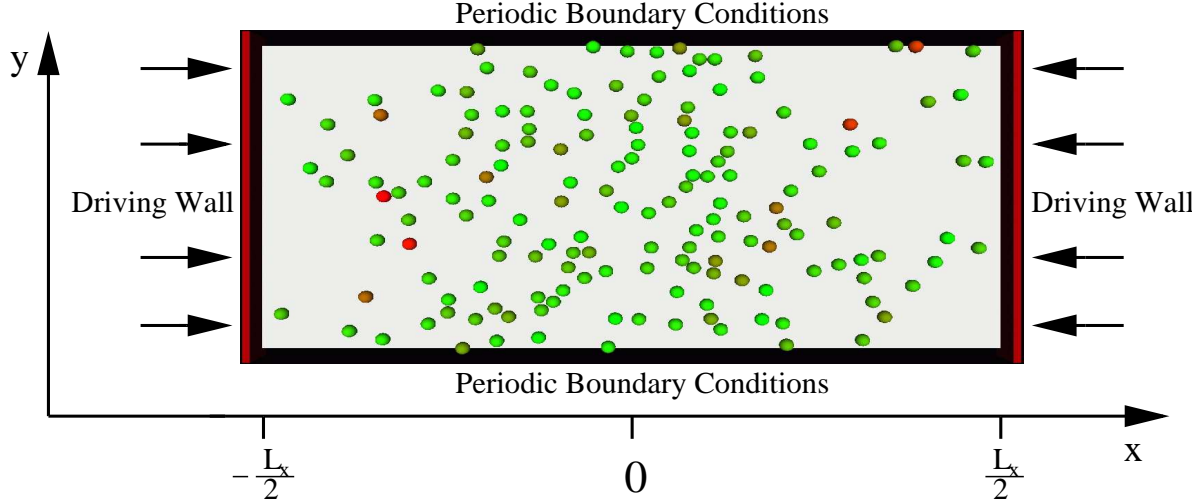


FIG. 1: Model of N disks, driven in the x -direction with periodic boundary conditions in the y -direction.

the collisional contribution to the heat current \mathbf{q}^{int} . For vanishing macroscopic velocity the energy balance equation is usually formulated as [6, 7]

$$\rho(\mathbf{r}, t) \frac{\partial}{\partial t} T(\mathbf{r}, t) = -\nabla \cdot \mathbf{q}(\mathbf{r}, t) + \zeta(\mathbf{r}, t) \quad (2)$$

for the hydrodynamic fields of density ρ , temperature T , total heat current $\mathbf{q} = \mathbf{q}^{\text{kin}} + \mathbf{q}^{\text{int}}$ and local energy dissipation rate ζ .

To compare our simulations to the hydrodynamic theory, we need to introduce a coarse graining function $\Phi(\mathbf{r})$ [13], which is nonzero in a small area centered at \mathbf{r} only. We require of course $\int d\mathbf{r} \Phi(\mathbf{r}) = 1$. In the absence of a velocity field, the coarse grained kinetic heat current is defined by

$$\mathbf{q}^{\text{kin}}(\mathbf{r}, t) = \sum_{i=1}^N \frac{m\mathbf{v}_i^2}{2} \mathbf{v}_i \Phi(\mathbf{r} - \mathbf{r}_i) . \quad (3)$$

The coarse grained density $\rho(\mathbf{r})$ and temperature $T(\mathbf{r})$ are defined analogously.

The change of energy during a binary collision in a small time interval Δt can be decomposed into a source term and a divergence of a flux. The coarse grained energy dissipation rate $\zeta(\mathbf{r}, t)$ can be calculated analogous to [13] and is given by

$$\zeta(\mathbf{r}, t) := \frac{1}{2\Delta t} \sum'_{i,j} (\Delta E_{i|j} + \Delta E_{j|i}) \Phi(\mathbf{r} - \mathbf{r}_i) \quad (4)$$

in terms of the change of energy $\Delta E_{i|j}$ of particle i due to a collision with particle j in the time interval $[t, t + \Delta t]$. The prime at the summation sign restricts i and j to those particles colliding in Δt . The energy dissipation rate trivially vanishes in the elastic case, when $\Delta E_{i|j} = -\Delta E_{j|i}$. Similarly, the collisional contribution to the heat current is given by

$$\begin{aligned} \mathbf{q}^{\text{int}}(\mathbf{r}, t) := & \frac{1}{4\Delta t} \sum'_{i,j} (\Delta E_{i|j} - \Delta E_{j|i}) \mathbf{r}_{ij} \\ & \times \int_0^1 \Phi(\mathbf{r} - \mathbf{r}_i + s\mathbf{r}_{ij}) ds , \end{aligned} \quad (5)$$

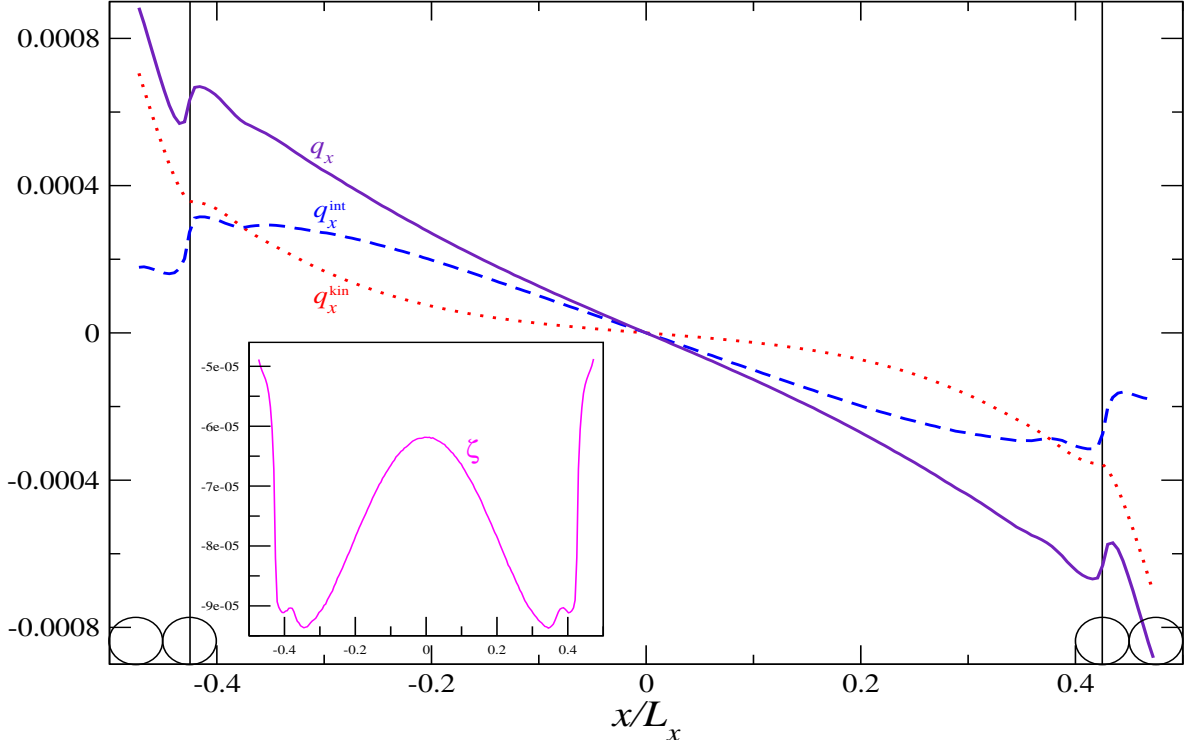


FIG. 2: The heat flux in the x -direction q_x for a system of $N = 256$ particles in a box of size $L_x = 20$ and $L_y = 25$, corresponding to a total area fraction of $\phi_0 = 0.4$. The dotted line shows the kinetic part q_x^{kin} , the dashed line is the collisional part q_x^{int} , and the full line represents the total heat flux q_x . The inset displays the local energy-loss rate ζ .

where $\mathbf{r}_{ij} = \mathbf{r}_i - \mathbf{r}_j$. In our simulations we have never found any significant variations of the long time averages of the hydrodynamic fields in the y -direction parallel to the driving walls. Hence we coarse grain our system by subdividing the box into stripes of width Δx .

In the following we report numerical results on the stationary state only. The reader who is interested in more details of the simulations, such as initialization or relaxation towards the stationary state, is referred to [12]. For dimensional reasons, the driving velocity v_0 sets the time and energy scale and is chosen to be 1. Likewise, the particle mass and diameter set the mass and length scales and are set to 1, too.

We first present data for the heat-flux profile in Fig. 2 for a system of global area fraction $\phi_0 := N\pi/(4L_xL_y) = 0.4$ and coefficient of normal restitution $\alpha = 0.9$. More precisely, the figure displays the x -component of the heat flux and its kinetic and collisional part as a function of the normalized position x/L_x . The inset shows the local energy-loss rate and will be discussed below. The heat flux is antisymmetric about the middle of the system as expected. We clearly see that its collisional part (5), which is represented by the dashed line cannot be neglected. It is of the same order as the kinetic contribution—depicted by the dotted line and corresponding to Eq. (3). For lower density systems the collisional contribution becomes less important but still it is not negligible for global area fractions even as low as $\phi_0 = 0.1$.

Now we turn to the dependence of the heat flux on the coefficient of restitution α in the elastic scaling limit. We recall that the driving strength has been adjusted such that the

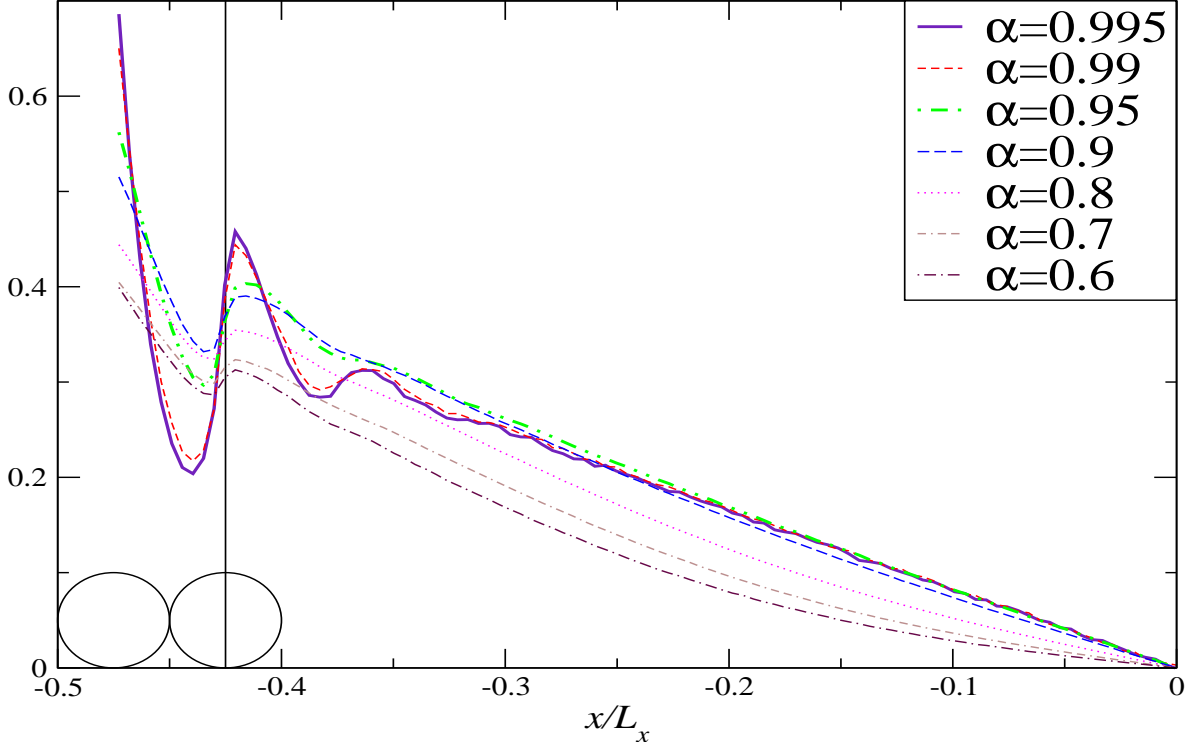


FIG. 3: Rescaled heat flux $(1 - \alpha^2)^{-1}(1 + \alpha)^{-2}q_x$ for a wide range of coefficients of restitution $0.6 \leq \alpha \leq 0.995$ for otherwise fixed systems ($L_x = 20$, $N/L_y = 10.24$ [$\phi_0 = 0.4$]).

granular gas attains a finite temperature as $\varepsilon \rightarrow 0$. The heat flux is proportional to the temperature per time and hence expected to scale like $T_0 v_{\text{drive}} \sim \varepsilon$, cf. (1). This argument is checked by plotting q_x/ε for different coefficients of restitution. The collapse of different data sets is excellent for almost elastic systems ($\varepsilon \ll 1$). With a slight modification of the scaling according to $q_x/[\varepsilon(1 + \alpha)^2]$, the data collapse also works approximately for the full range $0.6 < \alpha < 0.995$ and is shown in Fig. 3.

In Fig. 4 we show the heat flux for a fixed coefficient of restitution $\alpha = 0.99$ and various system sizes L_x . It has been shown [12] that the scale for temperature inhomogeneities is set by L_x , so that we expect the heat flux to scale like L_x^{-1} , if plotted versus x/L_x . In Fig. 4 we plot $q_x L_x$ for various system sizes L_x and get a decent data collapse for dilute systems. For higher densities this scaling captures at least the correct order of magnitude.

It is a characteristic feature of hydrodynamics of inelastically colliding particles that a heat current can be generated not only by a nonuniform temperature but also by density inhomogeneities. If the spatial variations of temperature or density are restricted to long wavelengths, one would expect a gradient expansion to hold. The simplest constitutive equation for the heat flux is thus a straightforward generalization of Fourier's law, as discussed in the literature, cf. [10]. Chapman–Enskog expansions of both the Boltzmann and the Boltzmann–Enskog equations predict that the heat flux of an inelastic system is given by

$$q_x(x) = -\kappa \frac{d}{dx}T(x) + \mu \frac{d}{dx}\rho(x) \quad (6)$$

where κ is the heat conductivity and μ is a new transport coefficient that has no analog for elastic systems [6, 7].

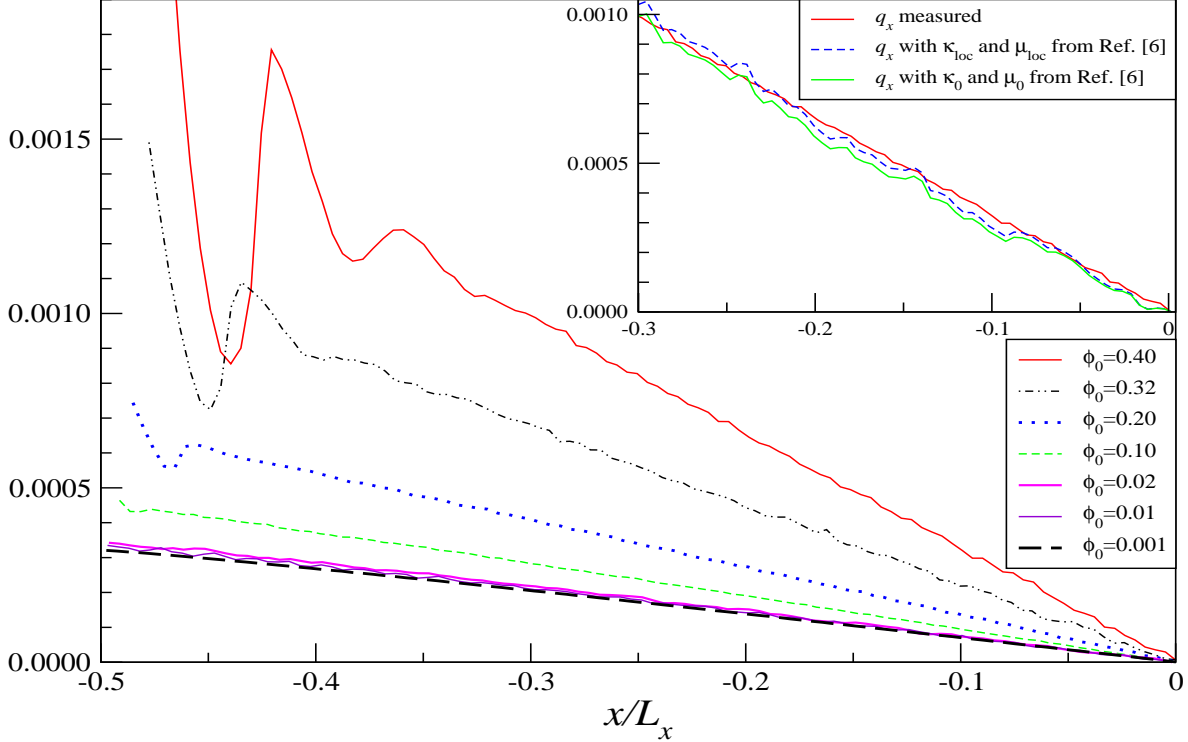


FIG. 4: Rescaled heat flux $L_x q_x$ for a wide range of box edges (area fraction $0.001 \leq \phi_0 \leq 0.4$ at fixed line density $N/L_y = 10.24$ and fixed coefficient of restitution $\alpha = 0.99$. This graph looks almost the same for all $\alpha \geq 0.9$.

To estimate the transport coefficients from our data, we assume that both, κ and μ , do not depend on the position x , i.e. we assume them to be constant throughout the box. It is then straightforward to extract them from a fit of our data to the above expression (6). In Fig. 5 we show both transport coefficients κ and μ/ε . Both are non-monotonic in α . In the elastic limit we find that κ tends to a non-zero constant, while $\mu \propto \varepsilon$. The fit of the heat flux as computed from Eq. (6) with constant κ and μ is very good for all investigated α , e.g. for $\alpha = 0.9$ it cannot be distinguished from the data shown in Fig. 2.

Both transport coefficients have been computed within kinetic theory for small inelasticities by Jenkins and Richman [6], who find for the thermal conductivity

$$\kappa = \left[\frac{2 + 3\phi\chi r^2(4r - 3)}{r\chi(17 - 15r)}(2 + 3\phi\chi r) + \frac{8\phi^2\chi r}{\pi} \right] \sqrt{\frac{T}{\pi}}, \quad (7)$$

where $r := (1 + \alpha)/2$. We use the Henderson approximation [14] for the pair correlation at contact χ which is a function of the area fraction only. Inserting the local temperature $T(x)$ and local area fraction $\phi(x)$ from our simulations into (7), we obtain a spatially dependent transport coefficient $\kappa_{\text{loc}}(x)$ and, from a corresponding equation in [6], $\mu_{\text{loc}}(x)$. The resulting heat flux from (6) is shown in the inset of Fig. 4 and found to agree very well with the simulations for $\alpha \geq 0.99$. The agreement is reasonable even up to $\alpha \sim 0.96$. For larger inelasticities the theoretical curves capture the correct order of magnitude, but overestimate the curvature of $q_x(x)$.

Alternatively we can use the global or mean temperature T_0 and area fraction ϕ_0 to

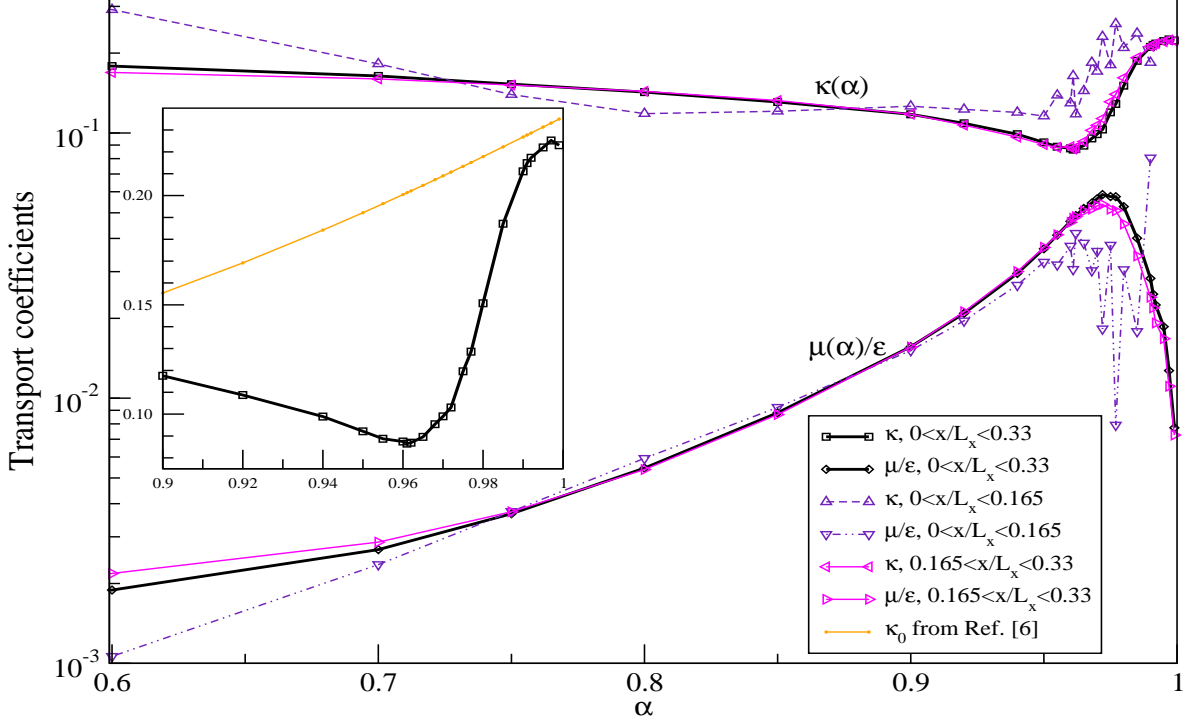


FIG. 5: Transport coefficients κ and μ as functions of the coefficient of restitution α for systems of size $L_x = 20$ and line density $N/L_y = 10.24$ ($\phi_0 = 0.4$).

evaluate Eq. (7) and the respective equation from [6] for μ . In Fig. 5 we compare this κ_0 to the thermal conductivity κ we obtained from fitting our simulations to Eq. (6). The agreement is good as long as $\alpha \geq 0.99$. As to μ_0 (not shown), the deviations to μ are quite strong. Note, however, that the theory of Ref. [6] as well as the simulations of Ref. [11] apply to the low density limit and not to $\phi_0 = 0.4$. Furthermore, the difficulties in our fitting procedure increase considerably as $\alpha \rightarrow 1$ because the temperature gradient becomes proportional to the density gradient. Consequently, it is not possible for $\alpha \rightarrow 1$ to determine two parameters from the fit unambiguously.

The difference between $\kappa_{\text{loc}}(x)$ and κ_0 is only a few percent for $\alpha \geq 0.99$. The difference in heat flux is even less, because the strongest inhomogeneities in the transport coefficients occur in the middle of the sample where the gradients of temperature and density vanish. The heat flux, computed using the constant transport coefficients κ_0 and μ_0 , is also shown in the inset of Fig. 4 for comparison. The fluctuations of the transport coefficients with x increase with increasing inelasticity, e.g. for $\alpha = 0.9$ we find $\kappa_{\text{loc}}(0)/\kappa \approx 1.5$.

To estimate the degree of inhomogeneity we have divided the box into an inner and an outer part and fitted the heat current using data from either half of the box only. The scattering of the data from the inner and outer part is shown in Fig. 5 and provides a rough measure for the effects of inhomogeneous transport. The results for the outer half are almost identical to the ones for the full system. This is also true for the inner part except for the weakly inelastic systems for which the absolute value of the heat flux in the middle of the sample is so small that statistical fluctuations dominate.

The local energy loss, as defined in Eq. (4), is shown in the inset of Fig. 2. Again, for $\alpha > 0.99$ the agreement with the predicted $\zeta = -16\varepsilon\phi^2\chi(T/\pi)^{3/2}$ from [6] is very

good (not shown). For very dilute quasi-elastic systems ($\phi_0 \lesssim 0.1$, $\alpha \gtrsim 0.95$) the dissipation is highest in the middle of the sample. For denser and/or more inelastic systems we find the absolute value of ζ (the dissipation) to be greatest in an intermediate region $x \sim \pm 0.3 L_x$. Even though the density is largest in the middle of the sample, energy dissipation is not very pronounced there because the mean kinetic energy is already comparatively small. Integrated over the whole box, the local energy loss has to fulfill the conservation law $q_x(-L_x/2) - q_x(+L_x/2) = \int_{-L_x/2}^{L_x/2} \zeta(x) dx$. This, of course, is confirmed in the simulations, but requires careful measurements of the heat flux at the boundaries.

In this paper we have discussed the heat current in a granular gas driven by vibrating walls. We have measured the collisional contribution to the heat current and have shown that it cannot be neglected, not even in low density systems. We have extracted transport coefficients, the thermal conductivity κ , as well as the transport coefficient μ , which accounts for a heat flux due to density inhomogeneities. Both transport coefficients have been determined for a wide range of inelasticities $0.6 \leq \alpha \leq 0.995$ and area fractions $0.01 \leq \phi_0 \leq 0.4$. We have studied in detail the elastic limit which is reached by scaling the driving velocity with ε , so that the temperature tends to a finite value as $\alpha \rightarrow 1$. Comparing our data to theoretical work in two dimensions [6] we found good agreement for $\alpha \geq 0.99$. For stronger inelasticities non-monotonic behavior is observed: The thermal conductivity κ first decreases with increasing ε , goes through a minimum around $\alpha \approx 0.96$ and then increases again. The transport coefficient μ/ε first increases with ε , goes through a maximum at $\alpha \approx 0.96$ and then decreases again. Furthermore a rough estimate of the fluctuations of the transport coefficients with spatial position in the box has been given. These effects are expected to be strong for moderately inelastic systems which are characterized by nonuniform density and temperature and need further investigation.

We thank Hans Vollmayr for pointing out to us the importance of the elastic limit and Isaac Goldhirsch for suggesting to measure the heat flux. We acknowledge financial support by the DFG through SFB 602, as well as Grant Nos. Zi 209/6-1 and Mu 1056/2-1.

-
- [1] T. P. C. van Noije and M. H. Ernst, *Granular Matter* **1**, 57 (1998).
 - [2] R. Caferio, S. Luding, and H. J. Herrmann, *Phys. Rev. Lett.* **84**, 6014 (2000).
 - [3] D. L. Blair and A. Kudrolli, *Phys. Rev. E* **67**, 041301 (2003).
 - [4] H. Hayakawa, *Phys. Rev. E* **68**, 031304 (2003).
 - [5] C. Bizon, M. D. Shattuck, J. B. Swift, and H. L. Swinney, *Phys. Rev. E* **60**, 4340 (1999).
 - [6] J. T. Jenkins and M. W. Richman, *Phys. of Fluids* **28**, 3485 (1985).
 - [7] J. W. Dufty, J. J. Brey, and A. Santos, *Physica A* **240**, 212 (1997).
 - [8] N. Sela and I. Goldhirsch, *J. Fluid Mech.* **361**, 41 (1998).
 - [9] J. T. Jenkins and C. Zhang, *Physics of Fluids* **14**, 1228 (2002).
 - [10] S. Chapman and T. G. Cowling, *The Mathematical Theory of Nonuniform Gases* (Cambridge University Press, London, 1970).
 - [11] R. Soto, M. Mareschal, and D. Risso, *Phys. Rev Lett.* **83**, 5003 (1999).
 - [12] O. Herbst, P. Müller, M. Otto, and A. Zippelius, *Phys. Rev. E* **70**, 051313 (2004).
 - [13] B. J. Glasser and I. Goldhirsch, *Phys. Fluids* **13**, 407 (2001).
 - [14] D. Henderson, *Molec. Phys.* **30**, 971 (1975).